Supporting Information

Post-translational succinylation of *Mycobacterium tuberculosis* enoyl-CoA hydratase EchA19 slows catalytic hydration of cholesterol catabolite 3-oxo-chol-4,22-diene-24-oyl-CoA

Amber C Bonds,[a] Tianao Yuan,[b] Joshua Werman, [b] Jungwon Jang,[b] Rui Lu,[b] Natasha M Nesbitt,[b] Miguel Garcia-Diaz,[a] Nicole S Sampson[b,]*

[a]*Department of Pharmacological Sciences, Stony Brook University, Stony Brook, New York 11794-*
[b]*Department of Chemistry, Stony Brook University, Stony Brook, New York 11794-3400*

*Corresponding author:
+1-631-632-7952 (phone)
+1-631-632-5738 (fax)
nicole.sampson@stonybrook.edu

Table of Contents

Table S1: Expression Constructs and Cloning Sites Used In This Work

Plasmid	Protein	Rv Number	Vector	Restriction Enzymes	His-tag Location	Antibiotic Selection
ChsE4-ChsE5 in pET28B	ChsE4-ChsE5	Rv3504-Rv3505	pET28B	*HindII & NdeI*	N-terminal	Kanamycin
EchA19$_{wt}$ in pET28B	EchA19$_{wt}$	Rv3516	pET28B	*HindIII & NdeI*	N-terminal	Kanamycin
EchA19$_{K139E}$ in pET28B	EchA19$_{K139E}$	Rv3516	pET28B	*HindIII & NdeI*	N-terminal	Kanamycin
EchA19$_{K132E}$ in pET28B	EchA19$_{K132E}$	Rv3516	pET28B	*HindIII & NdeI*	N-terminal	Kanamycin
EchA19$_{K132E\&K139E}$ in pET28B	EchA19$_{K132E\&K139E}$	Rv3516	pET28B	*HindIII & NdeI*	N-terminal	Kanamycin
EchA19$_{E137A}$ in pET28B	EchA19$_{E137A}$	Rv3516	pET28B	*HindIII & NdeI*	N-terminal	Kanamycin
Rv1151c in pET28B	Rv1151c	Rv1151c	pET28B	*HindIII & NdeI*	N-terminal	Kanamycin
FadD17 in pET28B	FadD17	Rv3506	pET28B	*HindIII & NdeI*	N-terminal	Kanamycin
MCR in 2BT	MCR	Rv1143	2BT	2BT vector-specific	N-terminal	Ampicillin

Table S2: Primer Sequences for Cloning and Protein Expression

Plasmid	Primers
ChsE4$_{wt}$-ChsE5 in pET28B	**F**: 5'-ATAATACATATGCGCATCAGTTACACCCCGCAGCAGGAGGAG-3'
	R: 5'-TATTATAAGCTTCTAGGCAGGGGTTTCCGCCAGTTCACGCGTCC-3'
EchA19$_{wt}$ in pET28B	**F**: 5'-GTGGGAATCCGGACCCG-3'
	R: 5'- GCCGCCAAGCTTCTAGCGGTTCTGGAAGTTGG-3'
EchA19$_{K139E}$ in pET28B	**F**: 5'-CTCCGAGGCCGAGTGGAGCCTGTACCC-3'
	R: 5'-GGGTACAGGCTCCACTCGGCCTCGGAG-3'
EchA19$_{K132E}$ in pET28B	**F**: 5'-CGGTGAAAGTGCGGAGTTCGGCATCTCCG-3'
	R 5'-CGGAGATGCCGAACTCCGCACTTTCACCG-3'
EchA19$_{K132E\&K139E}$ in pET28B	**F**: 5'-CGGTGAAAGTGCGGAGTTCGGCATCTCCG-3'
	R: 5'-CGGAGATGCCGAACTCCGCACTTTCACCG-3'
EchA19$_{E137A}$ in pET28B	**F**: 5'-TTCGGCATCTCCGCCGCCAAGTGGAGC-3'
	R: 5'-GCTCCACTTGGCGGCGGAGATGCCGAA-3'
Rv1151c in pET28B	**F**: 5'-TACTTCCAATCCAATGCAATGCGAGTGGCGGTGCTCAG-3'
	R: 5'-TTATCCACTTCCAATGTTATTACTATTTCAGCAGGGCGGGCAGG-3'
MCR in 2BT	**F**: 5'-TACTTCCAATCCAATGCAATGGCGGGTCCGCTGAGCGGGTT-3'
	R: 5'-TTATCCACTTCCAATGTTATTACTATCCGTCCCAGTCGGTGAGCACTGC-3'
FadD17 in pET28B	Primers mentioned previously[12]

Small-angle X-ray scattering of EchA19$_{wt}$ and EchA19$_{K139E}$ in solution. EchA19 Buffer C (20 mM Tris-HCl (pH 8), 300 mM NaCl) was used as the background solution for EchA19$_{wt}$ and EchA19$_{K139E}$ data collection. Small-angle X-ray scattering data sets were collected for both EchA19$_{wt}$ and EchA19$_{K139E}$ at varying concentrations: EchA19$_{wt}$ (0.25, 0.5, 1.0, 2.0 mg/mL) and EchA19$_{K139E}$ (0.25, 0.5, 1.0 mg/mL), respectively at the National Synchrotron Light Source (NSLS II) at Brookhaven National Laboratory (Upton, NY) on the Life Science X-ray Scattering (LiX) beamline, 16-ID. 60 µL of each sample and its matched buffer were exposed to X-rays for 6 min at 25 °C. The scattering contribution of the EchA19$_{wt}$ and EchA19$_{K139E}$ was obtained by subtracting the buffer scattering profile from the protein solution scattering profile. Scattering images collection and data reduction were performed using pyXS. The data were fit in GNOM to produce a well-behaved P(r) curve. SAXS data analysis was performed using the SasView small-angle scattering analysis software package (http://www.sasview.org/).

Table S3. Sphere model fitting parameters of EchA19$_{wt}$ and EchA19$_{K139E}$ small-angle X-ray scattering data.

Protein Sample	scale	scale_err	background	background_err	radius(Å)	radius_err
EchA19$_{K139E}$_0.25mg/mL	0.014046	0.000235	0.048475	0.004654	36.821	0.29007
EchA19$_{K139E}$ _0.5mg/mL	0.031563	0.000248	0.12061	0.004663	36.626	0.13618
EchA19$_{K139E}$ _1mg /mL	0.061917	0.000265	0.24439	0.004677	36.527	0.0744
EchA19$_{wt}$_0.25 mg/mL	0.00098	5.58E-05	0.002397	0.000946	36.639	0.96464
EchA19$_{wt}$_0.5mg/mL	0.002075	5.84E-05	0.004847	0.000946	36.468	0.47791
EchA19$_{wt}$_1mg/mL	0.004575	6.67E-05	0.008805	0.000999	36.164	0.24615
EchA19$_{wt}$_2mg/mL	0.009695	7.52E-05	0.014459	0.001019	35.967	0.13112

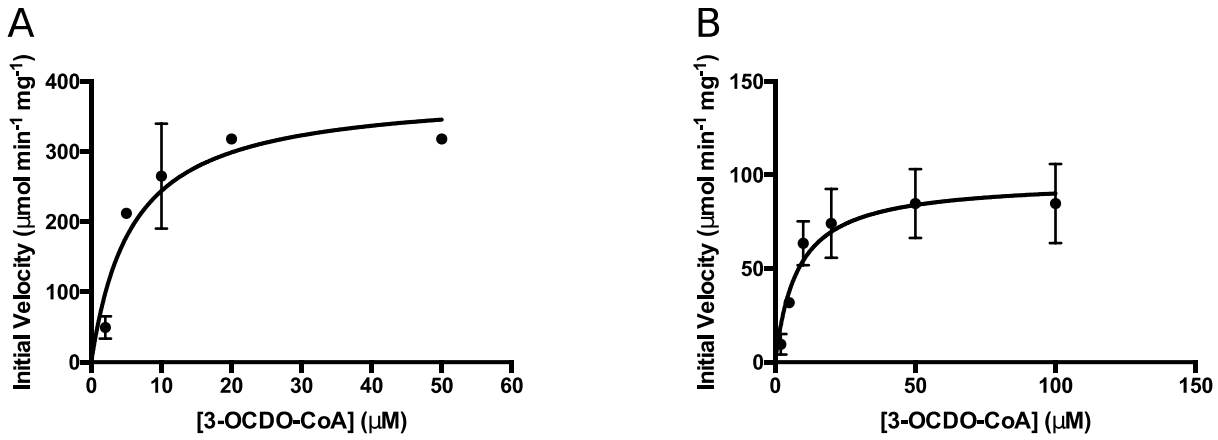

Figure S1. Michaelis-Menten plots for EchA19. Steady-state kinetic plots for (A) WT EchA19 and (B) succinylated EchA19 with 3-OCDO-CoA. The initial velocity is shown as a function of 3-OCDO-CoA concentration. The line represents a best fit of the Michaelis-Menten equation to the averaged data at each concentration. Three independent experiments were averaged.

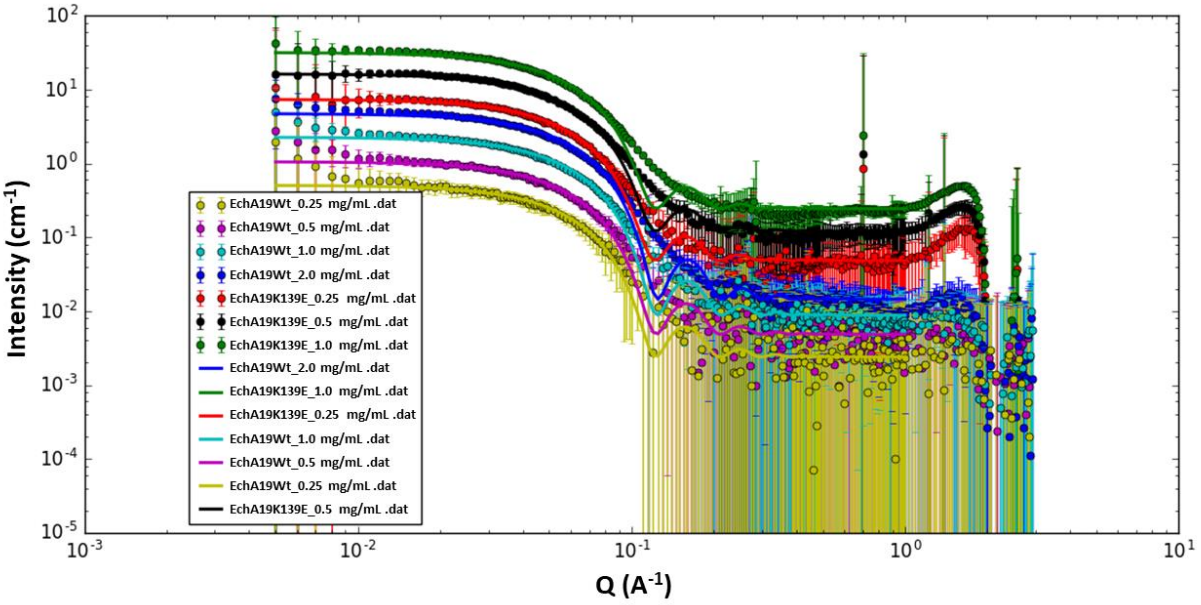

Figure S2. Small-angle X-ray scattering curves plotted for EchA19$_{wt}$ and EchA19$_{K139E}$. Small-angle X-ray scattering data for four EchA19$_{wt}$ samples and three EchA19$_{K139E}$ samples with different concentrations were fit to the sphere model. The background was subtracted from EchA19 Buffer C. The sphere model includes the radius R. For all protein samples, the radius was around 36 Å. The radius did not change with concentration or EchA19$_{wt}$ compared to EchA19$_{K139E}$, indicating that mutation of K139E in EchA19 did not result in structural changes.

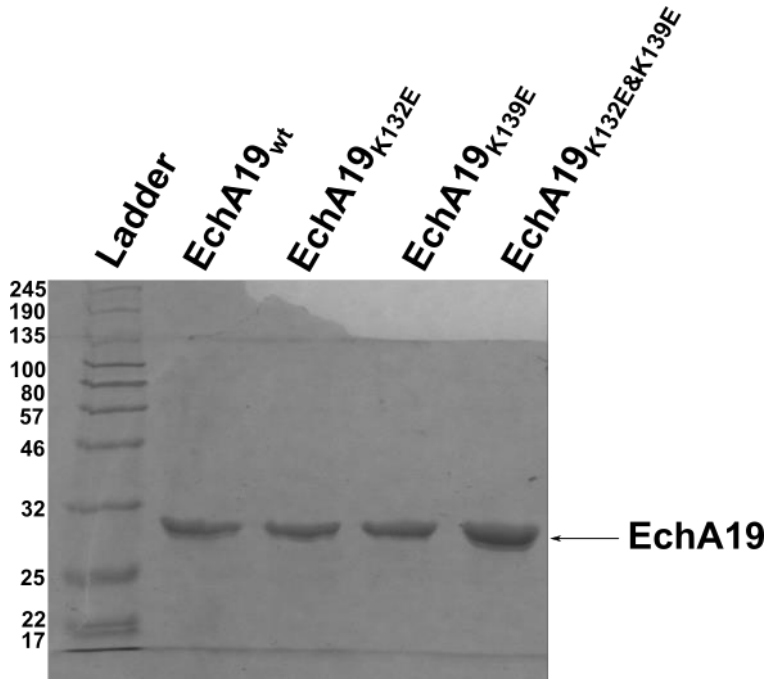

Figure S3. Gel purity of expressed proteins. SDS PAGE analysis of protein purity.